Supplementary Information

Micro Electronic Wireless Nitrate Sensor Network for Environmental Water Monitoring

Manas Ranjan Gartia, Björn Braunschweig, Te-Wei Chang, Parya Moinzadeh, Barbara S. Minsker, Gul Agha, Andrzej Wieckowski, Laura L. Keefer and Gang Logan Liu

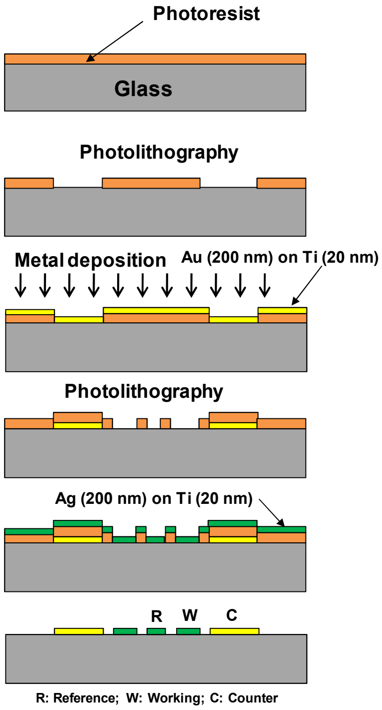

Figure S1: Fabrication steps for the micro sensor.

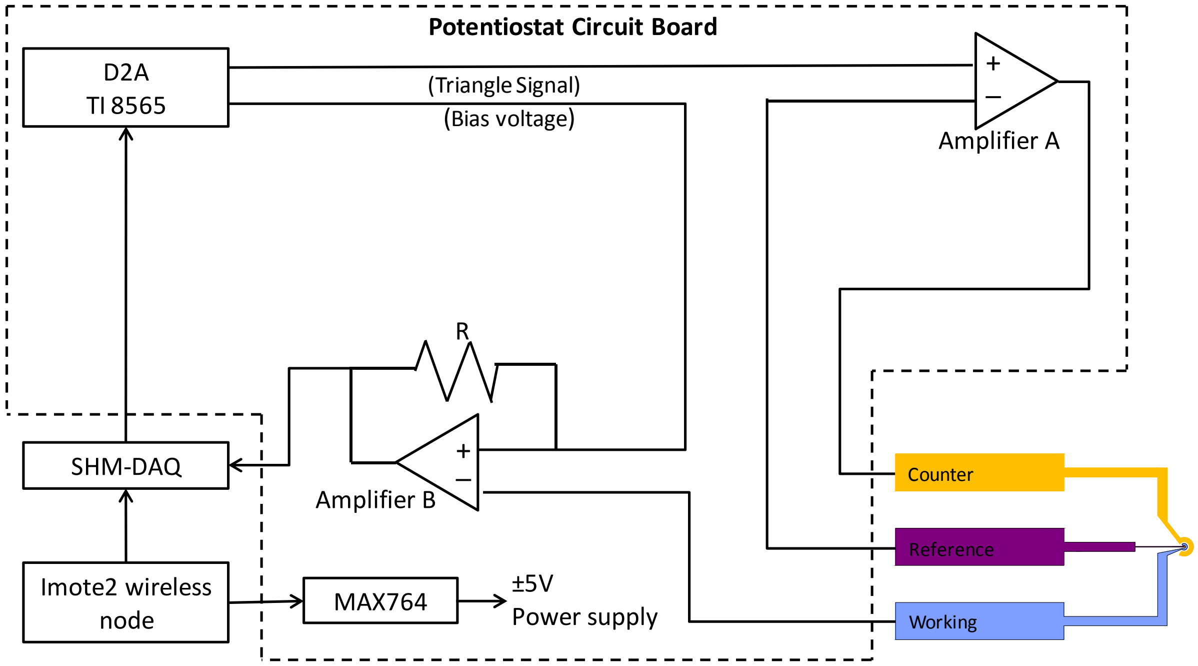

Figure S2: Schematic of circuit design for miniaturized potentiostat.

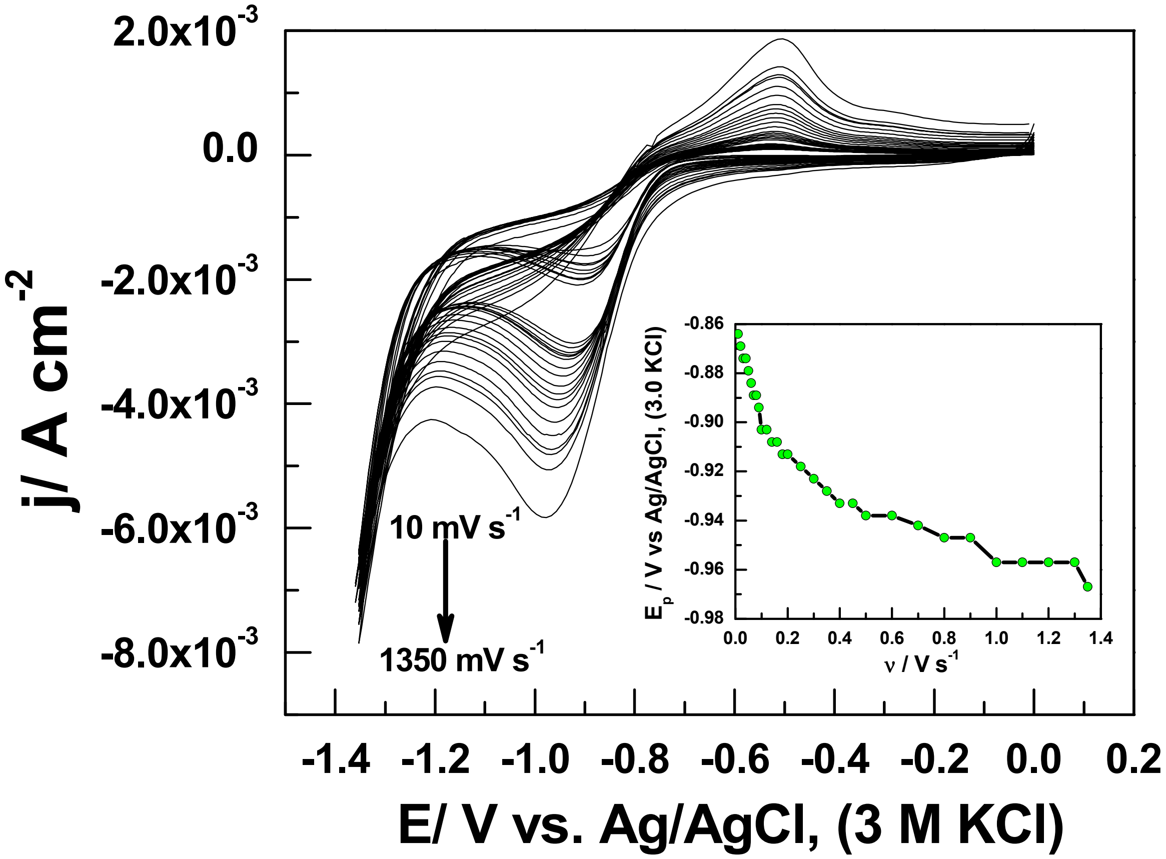

Figure S3: Cyclic voltammograms using a silver macro electrode in 10 mM NO_3^- and 0.1 M NaOH, with varying the scan rate from 10 to 1350 mV s^{-1}. Inset shows the variation of peak potential *vs.* scan rate.

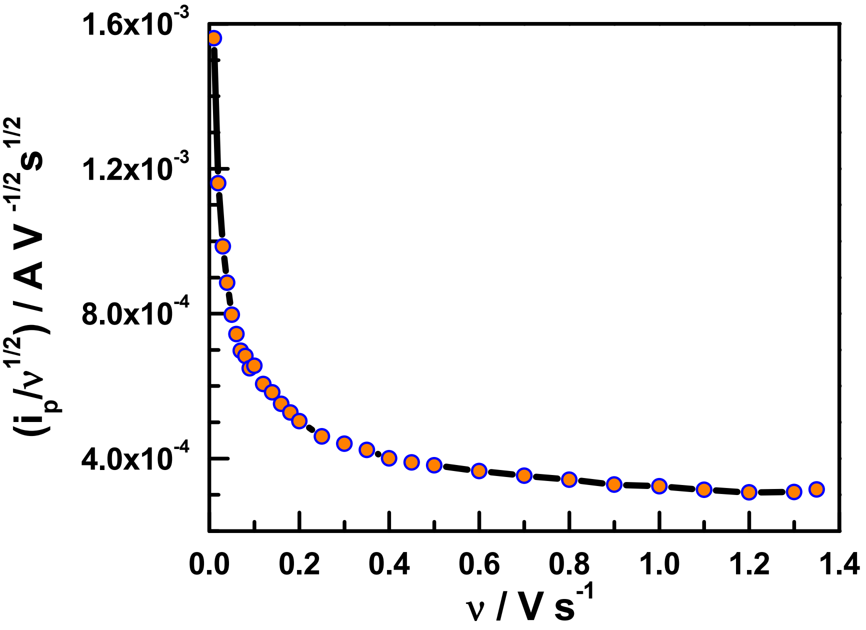

Figure S4: Variation of $i_p / v^{1/2}$ *vs.* scan rate for nitrate reduction on silver macro electrode in 0.1 M NaOH electrolyte.

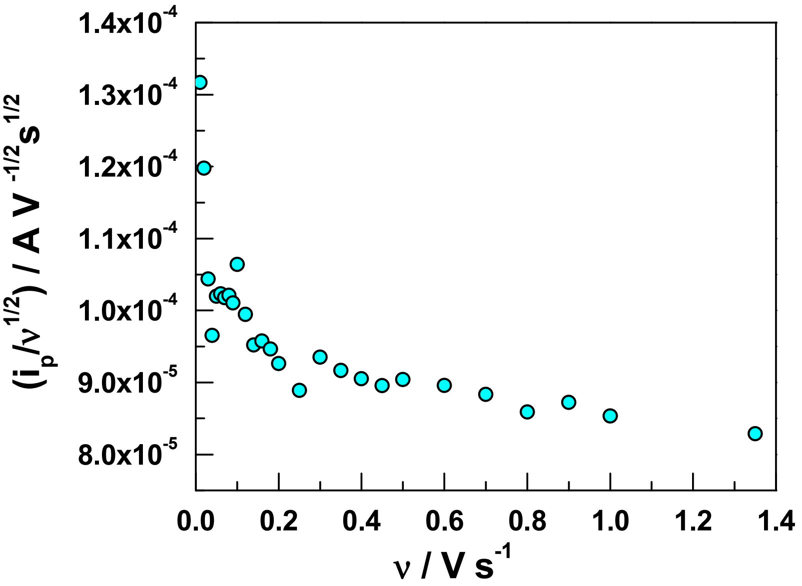

Figure S5: Variation of $i_p / v^{1/2}$ *vs.* scan rate for nitrate reduction using micro sensor in 0.1 M NaOH electrolyte.

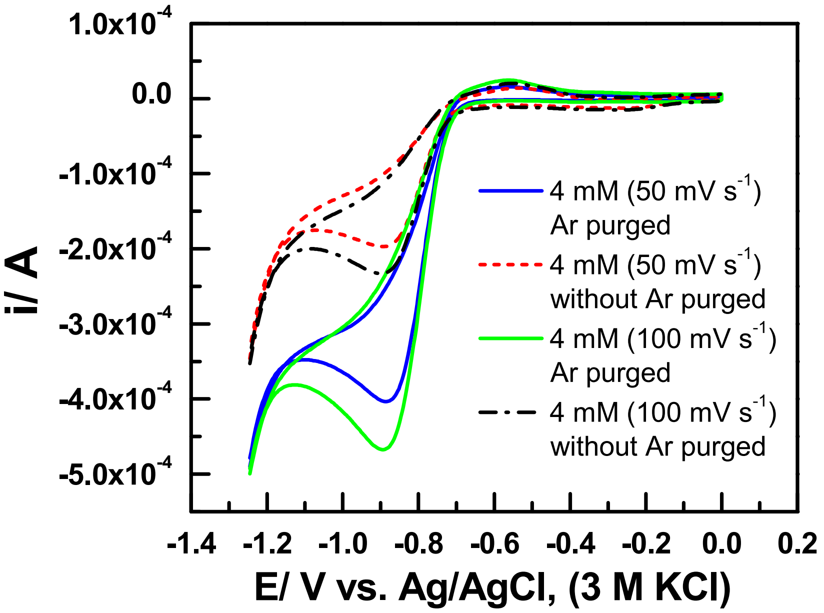

Figure S6: Cyclic voltammograms (50 and 100 mV s^{-1}) for the reduction of 4 mM nitrate in 0.1 M NaOH electrolyte with and without purging oxygen by argon.

a

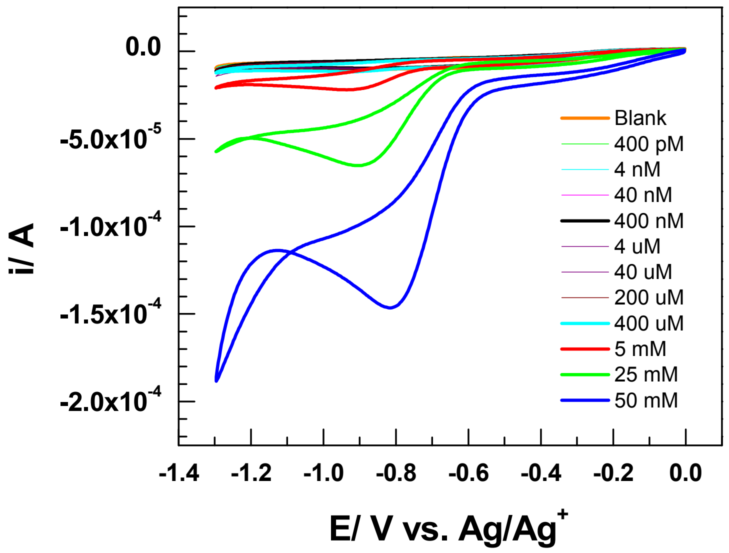

b

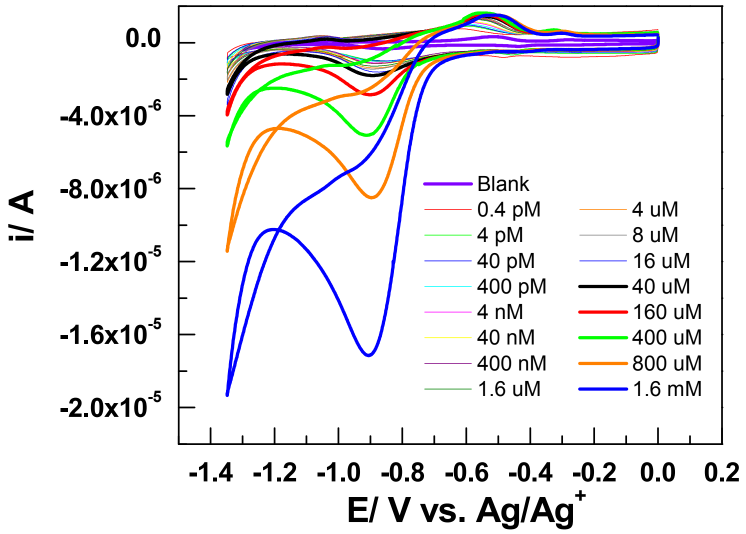

Figure S7: Cyclic voltammograms (50 mV s^{-1}) of nitrate with different concentration using micro sensor in a microfluidics. (a) Higher nitrate concentration (b) lower nitrate concentration.

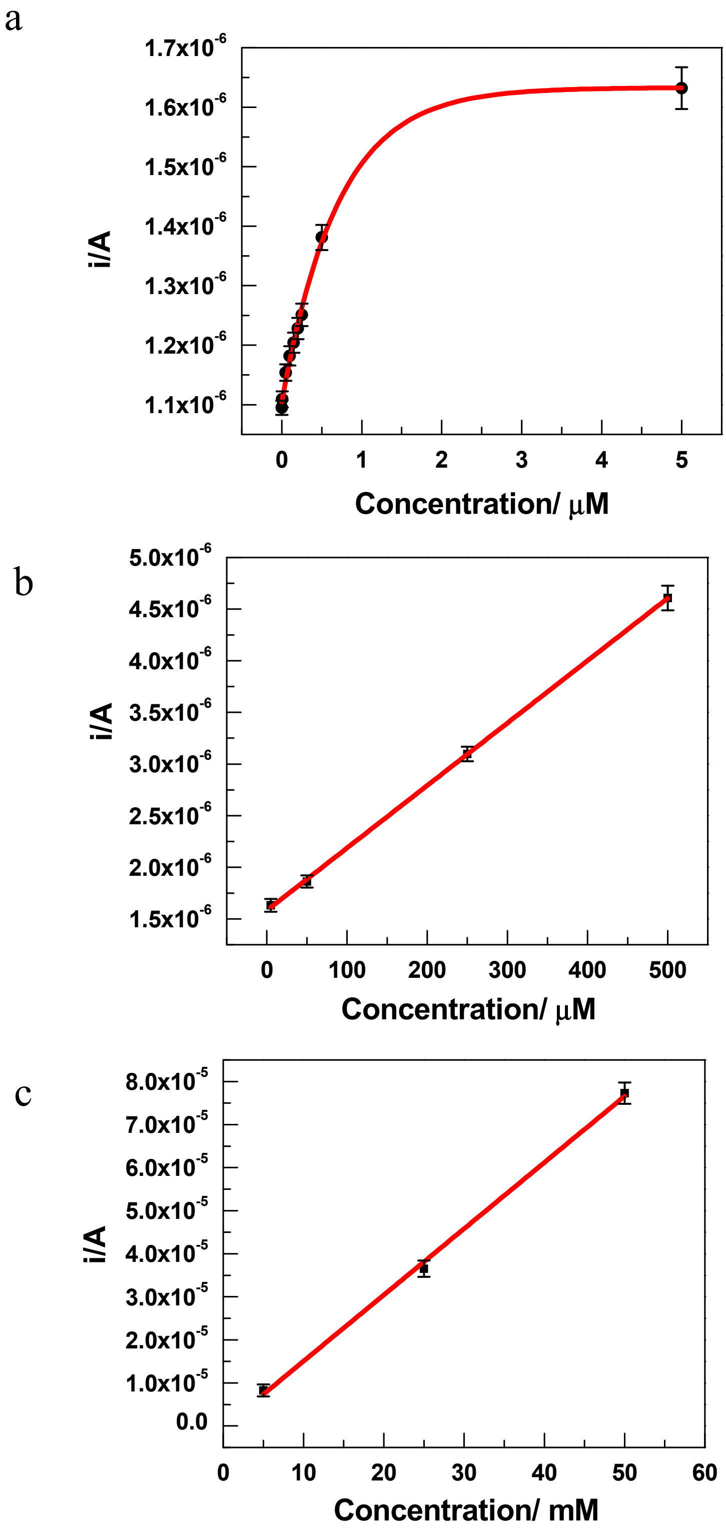

Figure S8: Calibration curves for nitrate using micro sensor in a microfluidics.

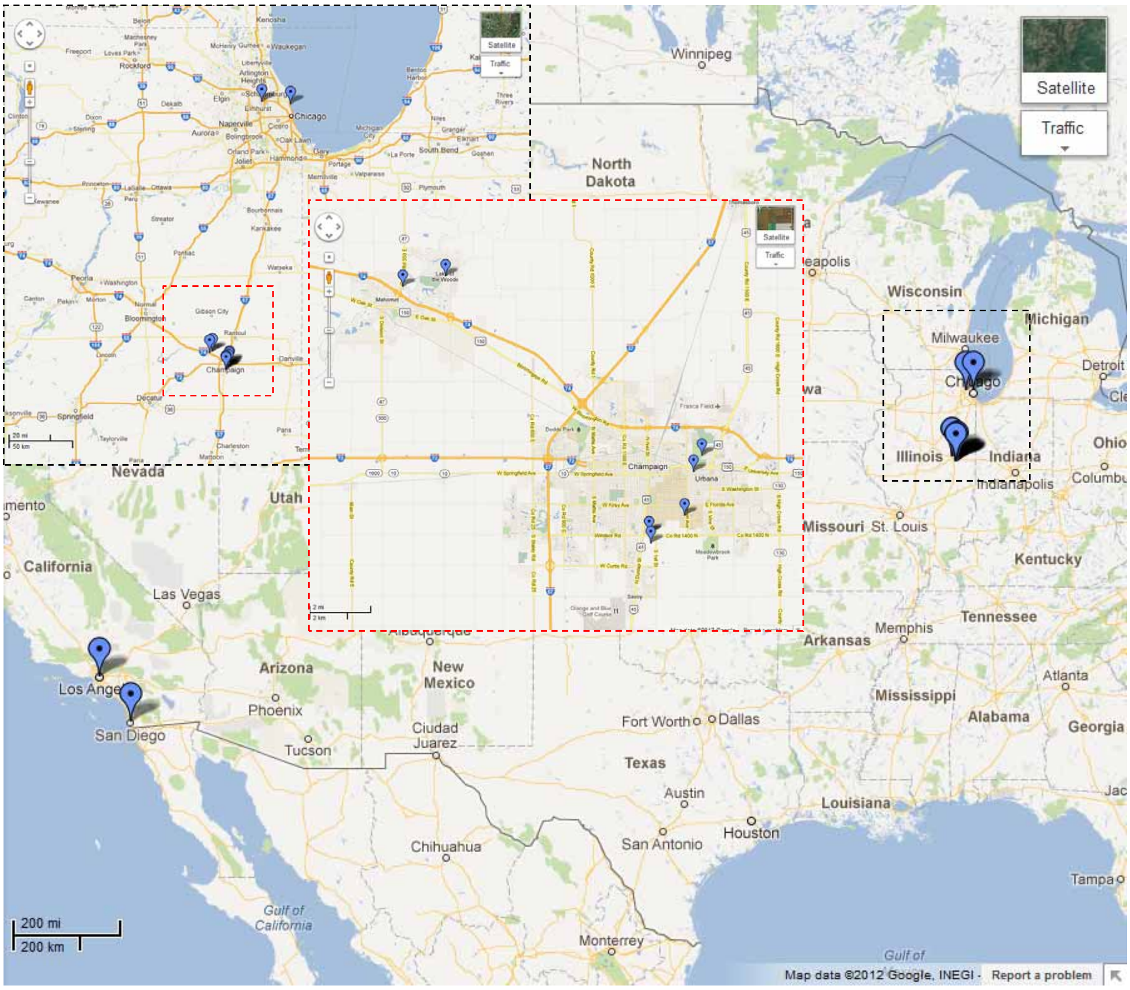

Figure S9: Location from which water samples collected are shown on google map

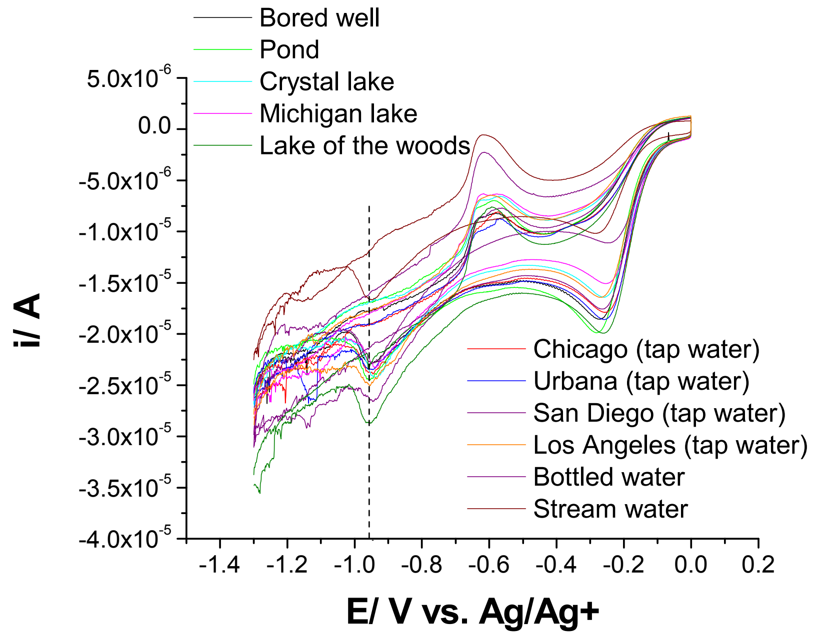

Figure S10: Electrochemical measurements of water samples using iNits.

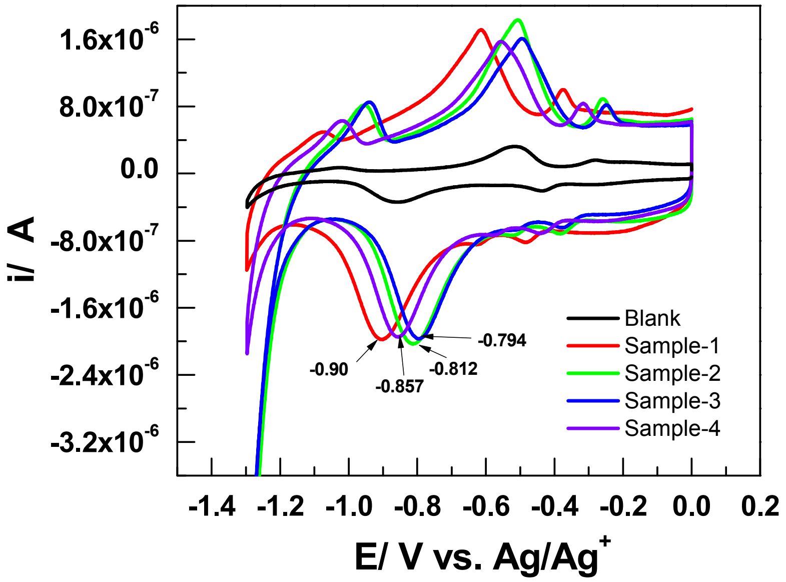

Figure S11: Cyclic Voltammetric determination of nitrate ions in water samples using micro sensor and microfluidics.

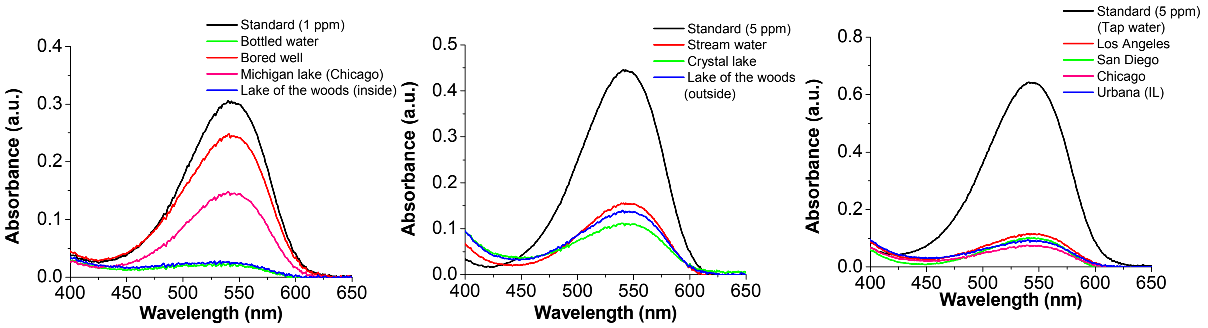

Figure S12: Nitrate reductase (NaR) method to determine the nitrate concentration. The absorbance peak at 543 nm is used for determining the nitrate-nitrogen concentration in water samples.

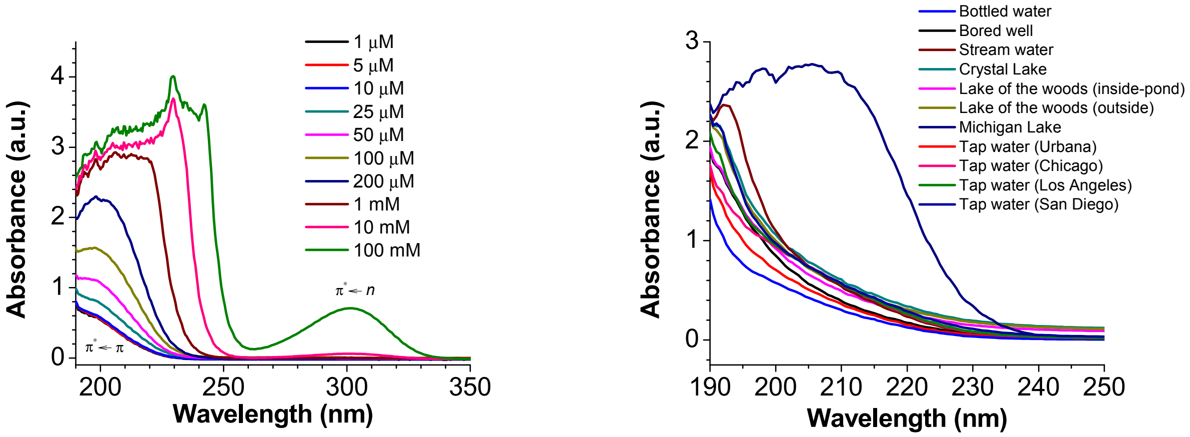

(a) Standard nitrate samples (b) Water samples

Figure S13: Ultraviolet screening method to determine the nitrate concentration. The absorbance peak at 200 nm is used for determining the nitrate-nitrogen concentration in water samples.

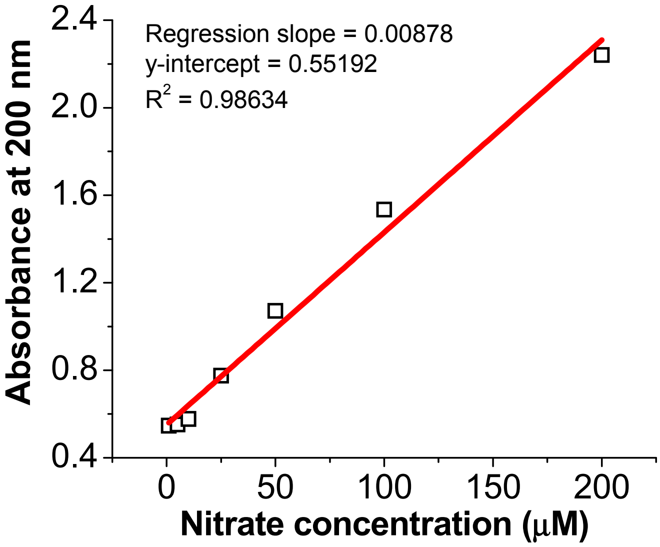

Figure S14: Calibration curve for the known concentration of nitrate standards.

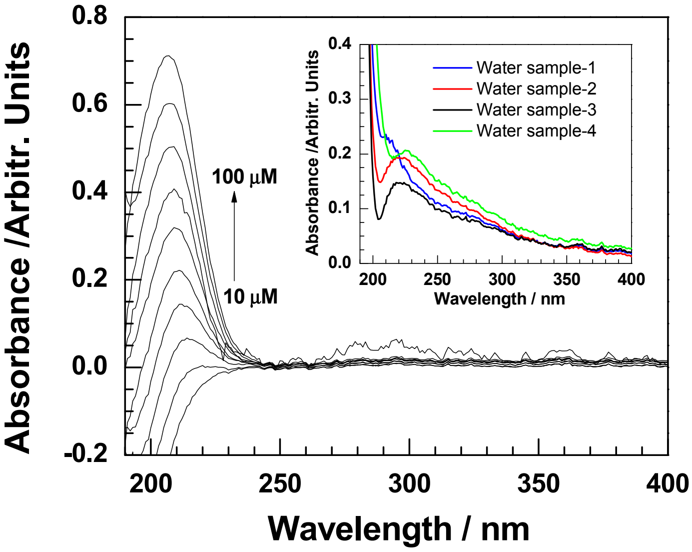

Figure S15: UV absorption spectra of nitrate with different concentration from 10 to 100 μM in DI water. The inset shows the UV absorption spectra of collected unknown water samples.

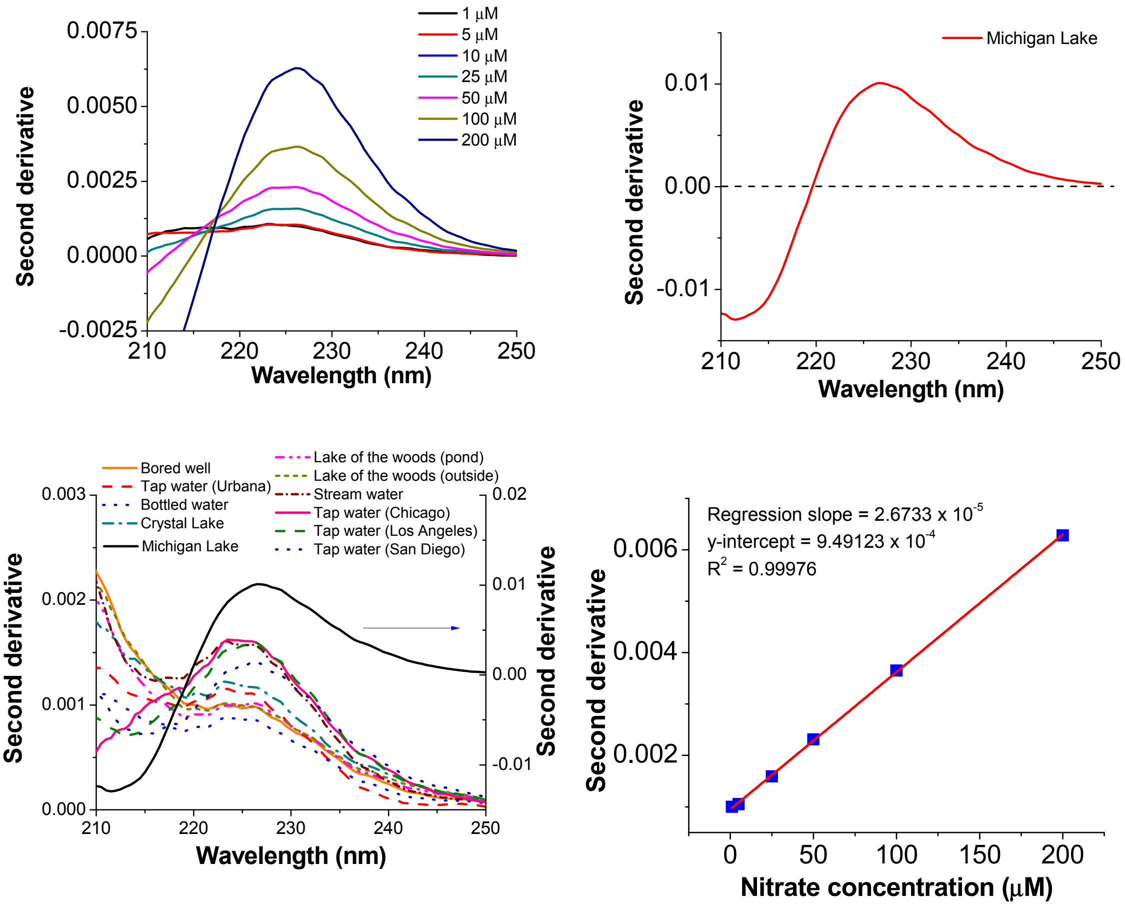

Figure S16: Second derivative Ultraviolet screening method to determine the nitrate concentration. The second derivative peak at 226 nm is used for determining the nitrate-nitrogen concentration in water samples.

Table S1: Water quality data of the water samples tested.

Samples	Location	Total hardness (ppm)	Total Chlorine (ppm)	Total Bromine (ppm)	Free Chlorine (ppm)	pH	Total Alkalinity (ppm)	Cyanuric acid (ppm)
Tap water	Chicago	100	0	0	0	7	80	40
	Urbana	100	1	2	1	8	150	40
	Los Angeles (LA)	100	0	0	0	7.8	180	30
	San Diego (SD)	250	0	0	0	8.4	180	40
Lake	Lake of the woods, Champaign	250	0.5	1	0	8.4	180	150
	Crystal lake, Champaign	250	0.5	1	0	8.4	240	100
	Michigan lake, Chicago	100	0.5	1	0	8.4	180	30
Bottled water	Nestle pure life	100	0	0	0	7.2	120	15
Bored well	Champaign, IL	500	0	0	0	8.4	180	40
Pond	Lake of the woods, Champaign	250	0	0	0	8.4	120	40
Stream water	Champaign, IL	500	0	0	0	8.4	240	40
	Sample-1, South campus, UIUC	400	0	0	0	8.0	200	40
	Sample-2, South campus, UIUC	500	0	0	0	8.2	120	40
	Sample-3, South campus, UIUC	400	0	0	0	8.4	200	40
	Sample-4, South campus, UIUC	450	0	0	0	8.0	240	40

Chemicals and apparatus

A 0.1 M nitrate stock solution was purchased from Thermo scientific. A silver-bulk electrode was prepared by sealing a 0.5 mm diameter 99.99% silver wire (Alfa Aesar, Ward Hill, MA, USA) in a glass tube using epoxy adhesive. The electrode surface was mechanically polished using commercial silver cleaner followed by 0.2 μm alumina powder. Ag/AgCl, NaCl (3.0 M), and a Pt wire were used as reference and counter electrodes, respectively. Cyclic voltammetry (CV) measurements on silver electrodes (bulk) and micro-sensor were carried out with an Autolab PGSTAT 100 potentiostat at room temperature. All measurements with the bulk electrode were performed under an argon atmosphere in an electrochemical cell with a 0.1 M NaOH (electrolyte) and 0.1 M H_2SO_4 liquid-liquid junction. The Ag electrode was electrochemically activated by cycling the potential from -1.3 to 1.0 V vs. a commercial Ag/AgCl reference with a scan rate of 1 V s^{-1} for 20 cycles.

Methods

Ultraviolet absorption spectroscopy

Ultraviolet (UV) absorption spectroscopy is also used to confirm and evaluate the nitrate concentration. In our experiment, a quartz cuvette containing the liquid sample was tested in an Evolution 60 UV-Visible Spectrophotometer for absorption measurement. For calibration of instrumental error, another cuvette with de-ionized water was used for reference. The scanning wavelength range is from 190 nm to 400nm, the scanning step is 1 nm and the integration time for each step is 1.5 seconds. We analyzed the collected water samples, and solution with different nitrate concentrations, shown in Figure S12, S13 and inset (of Figure S13). The measured UV absorption spectra of nitrate solution correspond to that in the literature [1, 2]. The absorption of known nitrate solution increases with the concentration while the shape of the absorption spectra remains the same. The absorption spectrum for nitrate solution showed two distinct peaks at the wavelength of 200-210 nm and 300 nm (this peak appears at concentrations higher than 1 mM only). We found that the absorption spectra of collected spring water samples are very similar to that of nitrate solution with distinct absorption peaks appearing at 200-220 nm. The nitrate concentration was determined from the calibration curve obtained using known concentration of nitrate standards.

Analysis of cyclic voltammetric (CV) data and comparison with bond dissociation free energy

The potential dependent free energy of activation for the nitrate reduction reaction can be written as a quadratic function of electrode potential as follows from Marcus's theory [3-7]:

$$\Delta G^{\dagger} = \Delta G_0^{\dagger}\left(1+\frac{\Delta G^0}{4\Delta G_0^{\dagger}}\right)^2 \tag{5}$$

where $\Delta G^0 = F\left(E-E^0\right)$, F is Faraday's constant, E^0 is the formal potential of the overall reaction and has a value of 0.01 V [8] and $\Delta G_0^{\dagger}$ is the intrinsic energy barrier for the reduction reaction[9]. The free energy of activation at the peak potentials corresponding to the cyclic voltammograms can be obtained by [10]:

$$\Delta G^{\dagger} = \frac{RT}{F}\left[\ln\left(Z\sqrt{\frac{RT}{F(\beta\times n)\nu D}}\right)-0.78\right] \tag{6}$$

where R is the gas constant, T is the temperature in K, $Z=\sqrt{\frac{RT}{2\pi M}}$ in cm s^{-1}, M is the molecular mass of nitrate and D is the diffusion coefficient in $cm^2\ s^{-1}$. $\beta\times n$ is calculated as[11]:

$$\beta\times n=\left(\frac{1.86RT}{F\left|E_p-E_{p/2}\right|}\right) \tag{7}$$

where E_p is the peak potential and $E_{p/2}$ is the potential when the current is half of the peak value. The resulting quadratic equation was solved for $\Delta G_0^{\dagger}$ using a MATLAB program. Finally, the bond dissociation free energy (BDFE) was calculated from the free energy of activation using the equation [7]

$$\Delta G_0^{\dagger}=\frac{R_0+R_i+BDFE}{4} \tag{8}$$

where the solvent reorganization energy, R_0, is calculated using Marcus equation as

$$R_0=\frac{e^2}{8\pi\varepsilon_0 a_0}\left(\frac{1}{\eta^2}-\frac{1}{\varepsilon_s}\right) \tag{9}$$

Here, η and ε_s are the refractive index and static dielectric constants of the solvent, respectively and a_0 is the effective radius of the analyte calculated by the equation [12]:

$$a_0=a_B\left(\frac{2a_{AB}-a_B}{a_{AB}}\right) \tag{10}$$

where $a_{AB}=a_{NO_3^-}=2.64\,\mathrm{A}^{o}$ and $a_B=a_{O^-}=1.76\,\mathrm{A}^{o}$. Neglecting internal reorganizational energy, R_i, (due to its small value) and substituting the earlier calculated value of $\Delta G_0^{\dagger}$ (intrinsic energy barrier for the reduction reaction) from Table S1, we can calculate the bond dissociation energy. For a nitrate concentration of 10 mM, scan rate of 0.01 Vs-1 and using an average diffusion coefficient of 1.9×10^{-5} cm^{2}s^{-1} [9], we have calculated the BDFE to be 47.2 kcal mol^{-1}, which matches well with the value of 47.5 kcal mol^{-1}, reported using photodissociation measurements [13] and theoretical studies [14].

Table S1 Analysis of cyclic voltammetric (CV) data for nitrate ion reduction (10 mM) using Micro sensor in microfluidics in 0.1 M NaOH

Scan rate/V s^{-1}	$10^5 I_p$/A	E_p/V	$(E_p\text{-}E_{p/2})$/V	$\Delta G_0^\dagger$ /kcal mol^{-1}
0.01	0.779	-0.874	0.065	22.71
0.02	0.972	-0.879	0.069	21.78
0.04	1.229	-0.879	0.072	20.89
0.08	1.601	-0.894	0.080	19.86
0.1	1.812	-0.903	0.082	19.44
0.2	2.334	-0.913	0.084	18.35
0.3	2.712	-0.923	0.087	17.67
0.4	3.121	-0.923	0.088	17.28
0.5	3.521	-0.933	0.090	16.83
1.0	4.835	-0.952	0.092	15.53

The calculated value of $\Delta G_0^\dagger$ is much greater than that expected for a step wise reduction of nitrate forming $NO_3^{\bullet 2-}$. Hence, in the current system, nitrate reduction is taking place in a concerted manner with NO_2^- and $O^{\bullet -}$ as intermediate products [9, 15]. The expected reduction reaction can then be written as [9]:

$NO_3^- + e^- \rightarrow NO_2^- + O^{\bullet -}$ (rate determining step)

$O^{\bullet -} + e^- + H_2O \rightarrow 2OH^-$

References

1. A. Ianoul, T. Coleman and S.A. Asher, *Anal. Chem.,* 2002**, 74***,* 1458-1461.
2. M.A. Ferree and R.D. Shannon, *Water Res.,* 2001**, 35***,* 327-332.

3. Marcus, R.A. On the Theory of Oxidation-Reduction Reactions Involving Electron Transfer .1. *J. Chem. Phys.* **1956,** *24,* 966-978.

4. Marcus, R.A. Electrostatic Free Energy and Other Properties of States having Nonequilibrium Polarization .1. *J. Chem. Phys.* **1956,** *24,* 979-989.

5. Marcus, R.A. Chemical + Electrochemical Electron-Transfer Theory. *Annu. Rev. Phys. Chem.* **1964,** *15,* 155-&.

6. Marcus, R.A. Exchange reactions and electron transfer reactions including isotopic exchange. Theory of oxidation-reduction reactions involving electron transfer. Part 4**.**—A statistical-mechanical basis for treating contributions from solvent, ligands, and inert salt. *Discuss. Faraday Soc.* **1960,** *29,* 21-31.

7. Saveant, J.M. Dissociative Electron Transfer, In *Advances in Electron Transfer Chemistry,* Mariano, P.S., Ed.; JAI Press: Greenwich, **1994**; Vol.4 pp. 53-116.

8. *Handbook of Electrochemistry.* Elsevier: Amsterdam, **2007**;

9. Bhat, M.A.; Ingole, P.P.; Chaudhari, V.R.; Haram, S.K. Mechanistic aspects of nitrate ion reduction on silver electrode: estimation of O-NO(2)(-) bond dissociation energy using cyclic voltammetry. *New Journal of Chemistry* **2009,** *33,* 207-210.

10. Pause, L.; Robert, M.; Saveant, J.M. Reductive cleavage of carbon tetrachloride in a polar solvent. An example of a dissociative electron transfer with significant attractive interaction between the caged product fragments. *J. Am. Chem. Soc.* **2000,** *122,* 9829-9835.

11. Bard, A.J. and Faulkner, L.R. *Electrochemical Methods: Fundamentals and Applications.* Wiley: New York, **2001**;

12. *Handbook of Chemistry and Physics.* CRC Press: New York, **1999**;

13. Kim, B. NO3, the Study of Molecular Properties and Photodissociation by Ab Initio Method, Spectroscopy, and Translational Spectroscopy. **1991,**

14. Zeng, X.; Chen, W.; Liu, J.; Kan, J. A theoretical study of five nitrates: Electronic structure and bond dissociation energies. *Journal of Molecular Structure-Theochem* **2007,** *810,* 47-51.

15. Broder, T.L.; Silvester, D.S.; Aldous, L.; Hardacre, C.; Crossley, A.; Compton, R.G. The electrochemical oxidation and reduction of nitrate ions in the room temperature ionic liquid [C(2)mim][NTf2]; the latter behaves as a 'melt' rather than an 'organic solvent'. *New Journal of Chemistry* **2007,** *31,* 966-972.